Numerical Simulation of Open Quantum Dynamics in a Trimon System: Impact of Master Equations and Charge Noise Modeling

Sadman Ahmed Shanto[1, *]

[1] *Department of Physics and Astronomy, University of Southern California*

In this work, we conduct an extensive numerical simulation study to analyze the effects of different master equations and charge noise modeling on the open quantum dynamics of a trimon system. We compare the predictions of the Lindbladian master equation (LME), Redfield master equation (RME), and Time-Convolutionless (TCL) master equations on the trimon's populations, coherences, and qubit state evolutions. Our study spans a range of initial density matrix states and various regimes of bath coupling strength and dephasing parameters. Furthermore, we also introduce a novel model for charge noise as a combination of amplitude and time-dependent phase damping. Our findings reveal interesting consistencies and discrepancies in the predictions of the master equations, with notable divergence in scenarios of strong dephasing amplitude. The TCL master equations, in particular, show potential implementation issues warranting further exploration.

I. INTRODUCTION

Quantum computing has garnered significant attention due to its potential to solve complex problems more efficiently than classical computing methods [1]. Qubits, the basic building blocks of quantum computing, are susceptible to various noise sources that can hinder the performance of quantum devices. Therefore, understanding and mitigating the effects of noise is crucial for the development of practical quantum computers [2].

Trimon systems, composed of three qubits, have recently attracted interest in the quantum information community as a platform for studying the effects of noise on quantum devices [3]. In this work, we investigate the dynamics of a trimon system under the influence of charge noise, a major source of decoherence in solid-state qubits [4]. Charge noise arises due to fluctuations in the electrostatic environment and can cause qubit energy levels to shift, which leads to decoherence [5].

We begin by introducing the trimon Hamiltonian and deriving a charge noise model. The noise model is then incorporated into a Lindblad Master Equation [6] to describe the system's dynamics. To further analyze the impact of charge noise on the trimon system, we employ both the Redfield-Bloch formalism [7] and the time-convolutionless (TCL) projection operator technique [8] to derive Master Equations, providing insight into the importance of higher-order contributions to the system dynamics.

In this paper, we present a detailed study of the open quantum dynamics of such a trimon system under the influence of various master equations and modeled charge noise. We compare the predictions of the Lindbladian Master Equation, the Redfield Master Equation, and the Time-Convolutionless Master Equations. Our simulations encompass various initial density matrix states, different regimes of bath coupling strength, and a range of dephasing parameters.

* shanto@usc.edu

II. TRIMON SYSTEM AND HAMILTON

A Trimon system is a multimode superconducting circuit that constitutes a key building block for scalable, programmable quantum processors. The Trimon system leverages the intrinsic features of superconducting circuits, such as high coherence times and strong anharmonicities, to enable coherent control over multiple frequency modes, paving the way for efficient quantum information processing and manipulation [9].

In typical superconducting architectures, the trimon system comprises three modes: a fluxonium qubit, a superconducting cavity, and a superinductor-based transmon, which are coupled via a superconducting quantum interference device (SQUID) [10]. The Hamiltonian of the Trimon system can be written as:

$$H = H_{\mathrm{flux}} + H_{\mathrm{cav}} + H_{\mathrm{trans}} + H_{\mathrm{int}}$$

where H_{flux}, H_{cav}, and H_{trans} represent the Hamiltonians of the fluxonium qubit, the superconducting cavity, and the superinductor-based transmon, respectively, and H_{int} represents the interaction Hamiltonian describing the coupling between these modes [9].

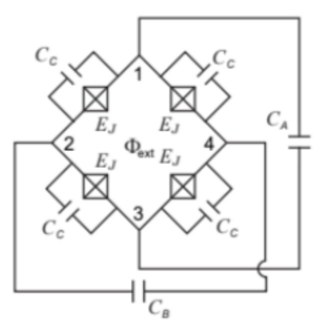

FIG. 1. Circuit Diagram of a trimon system using transmon qubits [9]

A crucial aspect of such systems is the ability to dynamically tune the coupling between the different modes, enabling selective coupling and decoupling for effective quantum gate operations. To achieve this, the SQUID is designed to have a tunable inductance, which can be controlled by an external magnetic flux. The tunability of the SQUID inductance allows the adjustment of the interaction Hamiltonian:

$$H_{\text{int}} = \sum_{i,j} g_{ij} a_i^\dagger a_j$$

where g_{ij} represents the coupling strength between modes i and j, and $a_i^\dagger$ and a_j are the creation and annihilation operators for the respective modes. By tuning the coupling strength between different modes, the Trimon system facilitates coherent control over multiple frequency modes, a key requirement for implementing programmable quantum processors [9].

In our work, we assume a simplified model of a trimonic system consisting of three interacting qubits, which can be described by a Hamiltonian of the following form:

$$H_{\text{trimon}} = \sum_{i=1}^{3} \frac{1}{2}\epsilon_i \sigma_z^{(i)} + \sum_{i<j} J_{ij}\sigma_z^{(i)}\sigma_z^{(j)}, \qquad (1)$$

where H_{trimon} is the system Hamiltonian, ϵ_i denotes the energy of the i-th qubit, $\sigma_z^{(i)}$ is the Pauli Z for the i-th qubit, and J_{ij} represents the coupling strength between the i-th and j-th qubits.

To study the open system dynamics of this trimon system, we need to introduce interactions between the system and its environment. In the next subsection, we introduce a charge noise model to describe this interaction.

A. Charge Noise Modeling in the Trimon System

In order to incorporate realistic charge noise in the Trimon system, we employ collapse operators that encapsulate relaxation and dephasing processes [11, 12]. These procedures are resultant from the interaction of the qubits with their environment, which are suitably captured using the Lindblad master equation approach, modeling open quantum system dynamics.

Two quintessential collapse operators for modeling charge noise include the amplitude damping (energy relaxation) and phase damping (pure dephasing) operators [11]:

- Amplitude Damping Operator (Energy Relaxation): This operator signifies the process where an excited qubit relaxes to the ground state due to environmental interactions. It can be formulated as follows:

$$\mathcal{A} = \sqrt{\gamma}\,|0\rangle\langle 1|,$$

where γ represents the relaxation rate.

- Phase Damping Operator (Pure Dephasing): This operator signifies the process in which a qubit loses its phase coherence due to environmental interactions, without changing energy. It can be represented as follows:

$$\mathcal{P} = \sqrt{\frac{\gamma_\phi}{2}}\,|1\rangle\langle 1|,$$

where γ_ϕ denotes the dephasing rate.

- Time-dependent Phase Damping Operator: A more realistic scenario could be to consider a fluctuating charge noise environment impacting the qubits. In this case, the dephasing rate becomes time-dependent, leading to a time-dependent collapse operator. Such a time-dependent dephasing rate can be modeled using a sinusoidal function:

$$\gamma_\phi(t) = \gamma_{\phi_0} + A\sin(2\pi f t),$$

where γ_{ϕ_0} is the base dephasing rate, A is the amplitude of the fluctuations, and f is the frequency of the fluctuations.

In our study, we model the charge noise as a process comprising both amplitude damping and time-dependent phasing damping. Thus, in the presence of charge noise, the system Hamiltonian becomes:

$$H_{\text{sys}} = H_{\text{trimon}} + H_{\text{noise}},$$

where H_{noise} models the charge noise in the system:

$$H_{\text{noise}} = \sum_i \xi_i(t) n_i$$

where n_i is the number operator for the i-th mode (associated with the amplitude damping), and $\xi_i(t)$ is a time-dependent stochastic process modeling the fluctuations in the charge environment (associated with the time-dependent phase damping).

In our case, we relax the stochastic process consideration and use $\xi_i(t) = A_i \sin(2\pi f_i t + \phi_i)$, where A_i is the amplitude of the noise, f_i is the frequency, and ϕ_i is a phase offset. This form allows the noise to have a certain frequency spectrum centered around f_i, as is often the case in realistic charge noise environments [13].

We use this noise model to derive the Lindbladian Master Equation (LME), Redfield Master Equation (RME), and the Time Convolutionless Master Equation (TCLME) - which are the focii of the rest of the paper.

III. LINDBLAD MASTER EQUATION

We know the Lindblad Master Equation is given by

$$\frac{d\rho}{dt} = -i[H, \rho] + \sum_k \gamma_k \left(A_k \rho A_k^\dagger - \frac{1}{2} A_k^\dagger A_k, \rho \right) \quad (2)$$

For our case with amplitude damping and time-dependent phase damping operators, the Lindblad Master Equation can be written as:

$$\frac{d\rho}{dt} = -i[H_{\text{sys}}, \rho] + \sum_{i=1}^{3} \big(2\sqrt{\gamma_i}\sigma_i^- \rho \sigma_i^+ - \{\sigma_i^+ \sigma_i^-, \rho\} + \\ 2\gamma_{\phi_i}(t)\sigma_{z_i}\rho\sigma_{z_i} - \{\gamma_{\phi_i}(t)\sigma_{z_i}^2, \rho\} \quad (3)$$

Here, ρ is the density matrix of the trimon system, σ_i^+ and σ_i^- represent the raising and lowering operators for the i-th qubit, and σ_{z_i} is the Pauli-z operator for the i-th qubit. γ_i is the amplitude damping rate for the i-th qubit, and $\gamma_{\phi_i}(t)$ is the time-dependent phase damping rate for the i-th qubit.

The LME describes the time evolution of the density matrix ρ considering both the unitary evolution and the effects of the environment in the form of amplitude and time-dependent phase damping (i.e. charge noise effects).

IV. REDFIELD MASTER EQUATION

For deriving the Redfield and TCL Master Equations, we need to define the bath and the system-bath interaction Hamiltonians:

$$H_B = \sum_k \hbar\omega_k (b_k^\dagger b_k + \frac{1}{2}) \quad (4)$$

where $b_k^\dagger$ and b_k are the creation and annihilation operators for the k-th mode of the bath with frequency ω_k.

$$H_I = \sum_{i=1} \sigma_z^{(i)} \otimes \sum_k g_k (b_k + b_k^\dagger)$$

We then transform this Hamiltonian into the interaction picture to separate the system and environment dynamics.

$$H_I(t) = e^{i(H_{sys}+H_B)t/\hbar} H_I e^{-i(H_{sys}+H_B)t/\hbar} \\ = e^{iH_S t} A e^{-iH_S t} \otimes B$$

where A and B are the system and bath operators, respectively.

The total time-evolution of the system is dictated by the Liouvillian superoperator, which, in the absence of system-environment interactions, reduces to the system Liouvillian, [11, 14] $L_S = -i[H_S, \cdot]$.

The Redfield tensor R is calculated by considering the influence of the environment on the system. This calculation involves finding the ensemble average of the correlation functions in the bath and integrating over all times [15]. For a system weakly coupled to a Markovian bath, the Redfield tensor can be approximated as

$$R = \sum_k \gamma_k(t) \left(2L_k \rho L_k^\dagger - L_k^\dagger L_k \rho - \rho L_k^\dagger L_k \right)$$

where $\gamma_k(t)$ are the relaxation rates and L_k are the Lindblad operators.

We further need to account for the bath's temperature by defining the spectral density of the bath, $J(\omega)$ (we assume an Ohmic Spectral Density), and the Bose-Einstein distribution, $n(\omega)$.

$$J(\omega) = \frac{2\alpha\omega}{\pi} \frac{\omega_c^s}{\omega_c^s + \omega^s}$$

where α is the coupling strength, ω_c is the cut-off frequency, and s is a parameter defining the type of spectral density ($s = 1$ for our case).

$$n(\omega) = \frac{1}{e^{\hbar\omega/k_B T} - 1}$$

where k_B is the Boltzmann constant and T is the temperature (we use 8 mK) of the bath.

We then incorporate the amplitude damping and phase damping operators, which describe the decoherence of the system due to its interaction with the environment.

The amplitude damping channel is described by the operator $L_a = \sqrt{\gamma(1 + n(\omega))}\sigma_-$, where γ is the damping rate and σ_- is the lowering operator. While, the phase damping channel is described by the operator $L_p = \sqrt{\gamma(t)n(\omega)}\sigma_z$, where $\gamma(t)$ is the time-dephasing rate and σ_z is the Pauli-z operator.

These operators are incorporated into the Redfield Master Equation to yield

$$\dot{\rho}(t) = -i[H_S, \rho(t)] + \sum_k \gamma_k(t) \left(2L_k \rho(t) L_k^\dagger - L_k^\dagger L_k \rho(t) - \rho(t) L_k^\dagger L_k \right) \quad (5)$$

where $\rho(t)$ is the system density matrix and the sum is over all the Lindblad operators, including the amplitude and phase damping operators. This equation describes the non-unitary evolution of the system due to its interaction with the environment.

V. TIME-CONVOLUTIONLESS (TCL) MASTER EQUATION

In our study we want to explore the non-Markovian dynamics of a quantum system interacting with its environment by utilizing the Time-Convolutionless (TCL) formalism [11]. The TCL method provides a more accurate description of the system-environment interaction, especially for non-Markovian dynamics, compared to other methods such as the standard Redfield equation that we derived in the previous section. The TCLN order master equation is derived by incorporating the N^{th}-order time-convolutionless projection operator expansion.

In this paper, we will primarily focus on studying the TCL2 ME (second order) and will provide a very general description on how to derive TCL4 ME.

A. TCL Order 1:

TCL1 is essentially the coherent evolution of the system without taking into account the system-bath interaction. Therefore, the TCL1 equation is simply:

$$\frac{d\rho(t)}{dt} = -i[H_S, \rho(t)] \tag{6}$$

where $\rho(t)$ is the reduced density matrix of the system.

B. TCL Order 2

Similar the the Redfield formalism, to derive TCL2 ME we start in the interaction picture.

$$H_{SB}(t) = \sum_i \sigma_z^{(i)} \otimes \sum_k \left(g_k e^{i\omega_k t} b_k + g_k^* e^{-i\omega_k t} b_k^\dagger \right)$$

Now, we want to calculate the time correlation functions of the environment, which are defined as:

$$C_{ij}(t) = \left\langle \left(\sum_k g_k e^{-i\omega_k t} b_k \right)_i^\dagger \left(\sum_k g_k e^{i\omega_k t} b_k \right)_j \right\rangle$$

For simplicity, we assume that the environment is in thermal equilibrium, and the time correlation functions are exponential:

$$C_{ij}(t) = \frac{\gamma_{ij}(t)}{2} \left(n(\omega_{ij}) + 1 \right) e^{i\omega_{ij} t} + \frac{\gamma_{ij}(t)}{2} n(\omega_{ij}) e^{-i\omega_{ij} t}$$

with $n(\omega_{ij})$ being the Bose-Einstein distribution function for the frequency ω_{ij}, and $\gamma_{ij}(t)$ represents the decay rates between energy levels i and j. Since, one of the decay rate (dephasing) is time-dependent in our model, we need to ensure that they are consistent with the bath operators.

We can calculate the bath correlation functions using the bath operators and the spectral density function as follows:

$$C_{\phi_i}(t) = \int_0^\infty d\omega J(\omega) \cos(\omega t) e^{-\omega/\omega_c}$$

where ω_c is the cutoff frequency, γ_{ϕ_i} it the time-dependent phase damping rates and $C_{\phi_i}(t)$ is the bath correlation function for the i-th qubit.

The time-dependent phase damping rates can be calculated as the time derivative of the bath correlation functions:

$$\gamma_{\phi_i}(t) = \frac{dC_{\phi_i}(t)}{dt}.$$

For the amplitude damping rate γ_i, we can use Fermi's golden rule to calculate the transition rate between energy levels:

$$\gamma_i = 2\pi J(\omega_i) |\langle e_i | \sigma_{z_i} | g_i \rangle|^2,$$

where $|e_i\rangle$ and $|g_i\rangle$ are the excited and ground states of the i-th qubit, and ω_i is the transition frequency between these two states.

Now, we want to compute the memory kernel $K(t-t')$, which involves convolving the time correlation functions. Recall that $K(t-t')$ represents the system's memory of its past states and is typically expressed as a matrix that depends on the time difference $t-t'$:

$$K(t-t') = \int_0^{t-t'} ds\, C(t-s) \tag{7}$$

Using this memory kernel, we set up the TCL master equation, which is an integro-differential equation for the reduced density matrix of the system:

$$\frac{d}{dt}\rho(t) = -i[H_S, \rho(t)] - \int_0^t ds\, [K(t-s)\rho(s), H_{SB}(s)] \tag{8}$$

Now, to actually solve Eq. (8) we employ the following pseudo-algorithm:

1. Compute the Laplace transforms of $K_{ij}(t-t')$ and $C_{ij}(t)$ to get $\tilde{K}_{ij}(s)$ and $\tilde{C}_{ij}(s)$
2. Compute $\tilde{\rho}(0)$ from $\rho(0)$ (Laplace transform) and $\tilde{\mathcal{D}}(s)$ from $\tilde{K}(s)$

$$\tilde{\mathcal{D}}(s) = \frac{\tilde{K}(s)}{s}$$

3. Compute the Liouvillian superoperator $\tilde{\mathcal{L}}(s)$ from $\tilde{\mathcal{D}}(s)$

$$\tilde{L}(s) = -i[H_S, \cdot] + \tilde{\mathcal{D}}(s)$$

4. Solve TCL 2 numerically (we used python -

```
scipy.linalg.solve(L_tilde(s),
rho_tilde(0))
```

) to get $\tilde{\rho}(s)$

$$\tilde{\rho}(s) = \frac{\tilde{\rho}(0)}{s} - \tilde{L}(s)\tilde{\rho}(s)$$

5. Compute $\rho(t)$ by taking the inverse Laplace transform of $\tilde{\rho}(s)$

C. TCL Order 4:

To derive the 4th order (TCL4) master equation using the TCL formalism [11], we need to expand the time-ordered exponential and consider up to the fourth-order terms. The TCL4 master equation will have the form:

$$\frac{d\rho(t)}{dt} = -\int_0^t dt_1 \int_0^{t_1} dt_2 \int_0^{t_2} dt_3 \, \mathrm{Tr}_B\{[H_{SB}(t), [H_{SB}(t_1), [H_{SB}(t_2), [H_{SB}(t_3), \rho_S(t_3) \otimes \rho_B]]]]\} \tag{9}$$

VI. CONNECTING TCL2 ME AND REDFIELD ME

$$\frac{d\rho(t)}{dt} = -\int_0^t dt_1 \, \mathrm{Tr}_B\{[H_{SB}(t), [H_{SB}(t_1), \rho_S(t_1) \otimes \rho_B]]\} \tag{10}$$

Using the general form of TCL2 ME Eq. (10), we can expand the double commutator and make use of the Born-Markov approximation, which assumes that the system and bath are only weakly coupled and that the bath returns to equilibrium much faster than the system evolves. This allows us to replace the $\rho_S(t_1)$ in the equation with $\rho_S(t)$ and assume that the integral over t_1 converges rapidly:

$$\frac{d\rho(t)}{dt} = -\int_0^t dt_1 \, \mathrm{Tr}_B\{H_{SB}(t)H_{SB}(t_1)\rho_S(t) \otimes \rho_B - H_{SB}(t)\rho_S(t) \otimes \rho_B H_{SB}(t_1) - H_{SB}(t_1)H_{SB}(t)\rho_S(t) \otimes \rho_B + \rho_S(t) \otimes \rho_B H_{SB}(t_1)H_{SB}(t)\} \tag{11}$$

Under the Born-Markov approximation, the above equation simplifies to a Lindblad master equation of the form:

$$\frac{d\rho(t)}{dt} = -i[H_S, \rho(t)] + \sum_k \gamma_k \left(L_k\rho(t)L_k^\dagger - \frac{1}{2}L_k^\dagger L_k\rho(t) - \frac{1}{2}\rho(t)L_k^\dagger L_k \right) \tag{12}$$

where $\rho(t)$ is the reduced density matrix of the system, γ_k are the decay rates, and L_k are the Lindblad operators (also known as jump operators).

To derive the TCL2 Redfield equation, we need to rewrite the interaction-picture interaction Hamiltonian $H_{SB}(t)$ in terms of the system operators A_k and bath operators B_k:

$$H_{SB}(t) = \sum_k (A_k \otimes B_k)(t) \tag{13}$$

Substituting this expression into the TCL2 master equation and using the Born-Markov approximation, we arrive at the Redfield equation:

$$\frac{d\rho(t)}{dt} = -i[H_S, \rho(t)] + \sum_{k,l} (R_{kl}A_k\rho(t)A_l^\dagger - \frac{1}{2}A_l^\dagger A_k\rho(t) - \frac{1}{2}\rho(t)A_l^\dagger A_k) \tag{14}$$

Where R_{kl} are the Redfield tensor elements, given by:

$$R_{kl} = \int_0^\infty dt \, e^{i\omega_{lk}t} \left(C_{kl}^+(t) + C_{kl}^-(t) \right) \tag{15}$$

$\omega_{lk} = \omega_l - \omega_k$, and $C_{kl}^\pm(t)$ are the bath correlation functions.

VII. SIMULATIONS

In this section, we present the results of our numerical simulations of the open system dynamics of our trimon system. Our primary focus is to study the populations, coherences, and Bloch sphere evolutions of the qubits under different master equations. By comparing these results, we aim to gain insights into the relative strengths and weaknesses of different master equations in predicting the open quantum dynamics of a trimon system. Such a systematic comparison will not only validate our simulation framework but also contribute to the broader understanding of open quantum systems

The primary parameters of our simulations include the Hamiltonian of the system, the system-bath coupling operators, and the spectral density of the bath. For the system-bath coupling operators, we have accounted for the interaction of each of the three qubits in the trimon system with the bath (kept constant across the various models). We model the spectral density of the bath using the Ohmic spectral density function.

The simulation codebase has been made public and can be found here - https://github.com/shanto268/trimon_oqs.

Unfortunately, due to the time constraints set by our project deadline, we could not use the TCL2 algorithm defined earlier to compute the dynamics - its implementation was/is not optimized for the time range of interest because of high computational cost of the routine.

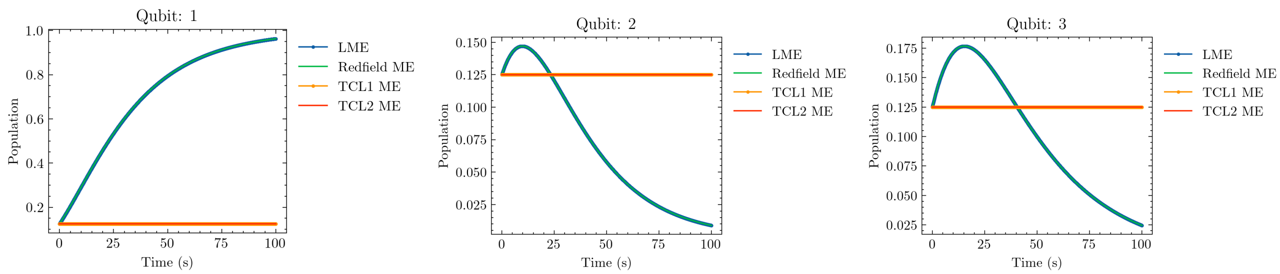

FIG. 2. From left to right: Populations in Qubit 1, 2 and 3

Instead, we used the HEOM method to implement the TCL2 in simulation.

In this HEOM approach, one solves the dynamics and steady state of a system and its environment, the latter of which is encoded in a set of auxiliary density matrices. The Bosonic environment is implicitly assumed to obey a particular Hamiltonian in this approach [16], the parameters of which are encoded in the spectral density, and subsequently the bath correlation functions.

Moreover, the API of ‘qutip‘ (an opensource package in python) restricts us to only use Drude-Lorentz Spectral Density. We found a clever solution through a tutorial inspired by [17–19] which allowed us to use a set of underdamped brownian oscillator functions with Drude-Lorentz Spectral Density and Matsubara decompositions [17, 20] to approximate our Ohmic Spectral Density for the overall bath within the constraints of the API.

A. Results

Through our simulations we observe an intriguing phenomenon. The Lindbladian master equation (LME) and the Redfield master equation (RME) concur in their predictions for the evolution of trimon's populations, coherences, and qubit dynamics (characterized in the Bloch sphere representation) as seen in **Figures [2, 4, 3]**. This is an interesting outcome, considering that both approaches are predicated on different approximations.

On the other hand the Time-Convolutionless (TCL) approach, reveals a discrepancy. While both TCL1 and TCL2 predictions align with each other they don't with LME and RME in terms of population dynamics; further, they diverge in their predictions for coherences and Bloch sphere evolutions (**Figures [2,5,3]**).

The discrepancy with the TCL2 results is particularly noteworthy, as the coherences exceed $\pm$ unity during the course of the simulation. This is physically implausible as it violates the bounds of the coherence. This strongly suggests an implementation error in the TCL2 method, which warrants further investigation.

However, the TCL1 result seems plausible as it reflects essentially unitary evolution, which is expected in the absence of a bath or any external influences.

The initial state of the transmon system in this simulation was the product superposition state -

$$|\psi(0)\rangle = \frac{1}{\sqrt{2}}\left(|0\rangle + |1\rangle\right) \otimes \frac{1}{\sqrt{2}}\left(|0\rangle + |1\rangle\right) \otimes \frac{1}{\sqrt{2}}\left(|0\rangle + |1\rangle\right)$$

To further corroborate our observations, the simulations were repeated for various initial density matrix states, including the W state, Bell state, maximally entangled states, one qubit excited states, and Greenberger-Horne-Zeilinger (GHZ) states. The patterns observed in the case of the trimon system held true across these different initial states. The LME and RME consistently yielded congruent predictions for populations, coherences, and qubit dynamics, whereas the TCL1 and TCL2 approaches differed in their predictions for coherences and Bloch sphere evolutions.

Further, we examined the effects of bath coupling strength and dephasing parameters on these dynamics. The simulations were performed in different regimes of bath coupling strength and varying dephasing parameters. Intriguingly, the agreement between the different master equation's predictions persisted across these variations, further strengthening the robustness of our initial observations or more likely demonstrating the same source of systematic errors.

However, a departure from this trend was observed in the case of very strong amplitude of dephasing. In this specific instance, the LME and RME predictions for coherences and Bloch sphere evolution diverged **(Figures [6, 7])**, although their predictions for populations remained in agreement. This discrepancy suggests that the Markovian approximation inherent in the LME may break down under conditions of strong dephasing, leading to deviations from the non-Markovian RME predictions. It is also plausible that under these extreme conditions, the system-bath correlations become significant, thus affecting the dynamics in a way that is not captured by the second-order RME. Further investigation is required to elucidate the underlying causes for this divergence in the strong dephasing regime.

VIII. CONCLUSION

In conclusion, we introduced a novel charge noise model to the trimon to study its open system dynam-

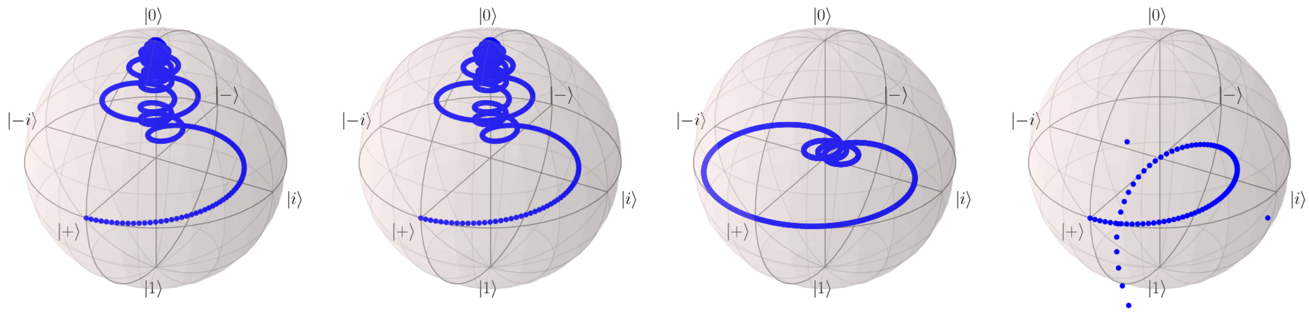

FIG. 3. From left to right: LME, Redfield ME, TCL1 ME, TCL2 ME

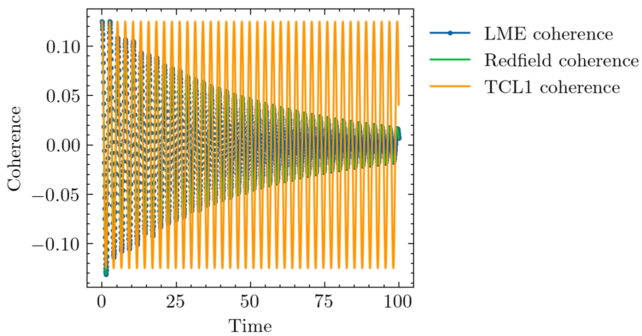

FIG. 4. Coherences without TCL2 ME

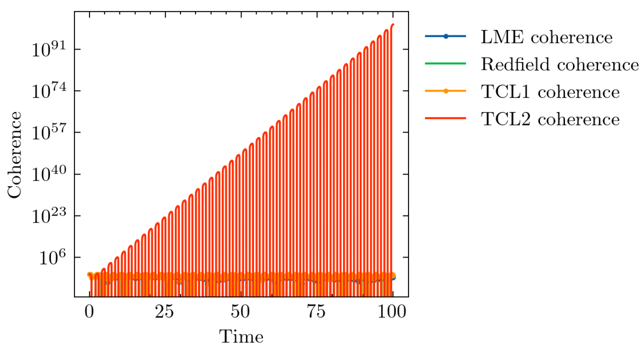

FIG. 5. Coherences with TCL2 ME

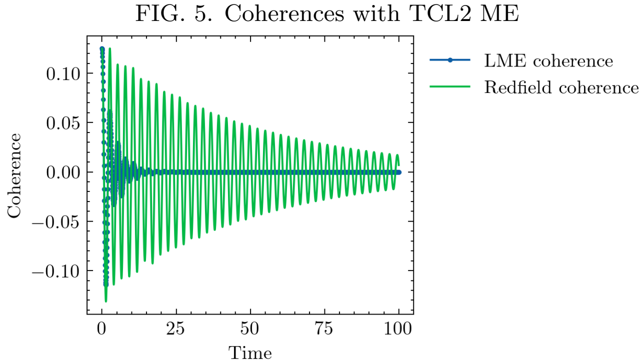

FIG. 6. Coherences under strong dephasing amplitude

ics, though further work is needed to refine it. Furthermore, we also presented a comprehensive study of this open quantum dynamics using numerical simulations; We explored the predictions of different master equations—namely, the Lindbladian master equation (LME), Redfield master equation (RME), and Time-Convolutionless (TCL) master equations—for the trimon's populations, coherences, and qubti state evolutions. We observed interesting consistencies and discrepancies in these predictions, thereby highlighting the comparative strengths and weaknesses of these master equations.

The LME and RME displayed congruence in their predictions across a range of initial density matrix states and varying bath coupling strengths and dephasing parameters - notably diverging in the strong dephasing amplitudes. The TCL master equations, while consistent with each other in terms of population dynamics, diverged from the LME and RME predictions in their treatment of coherences and Bloch sphere evolutions. In particular, the TCL2 master equation yielded physically implausible coherence values, suggesting a possible implementation error.

Despite these results, we strongly urge readers to interpret these findings with caution and skepticism. There are several limitations to our study that could impact the validity of our results. The methodological constraints owing to our simulation package may have introduced systematic errors that could undermine the generalizability of our findings.

Future work should strive to address these limitations, possibly starting with optimizing the TCL2 algorithm for greater computational efficiency. Our hope is that such enhancements will enable more accurate and robust simulations of open quantum dynamics, thereby advancing our understanding of these complex systems.

[1] M. A. Nielsen and I. L. Chuang, *Quantum Computation and Quantum Information* (Cambridge University Press, 2010).

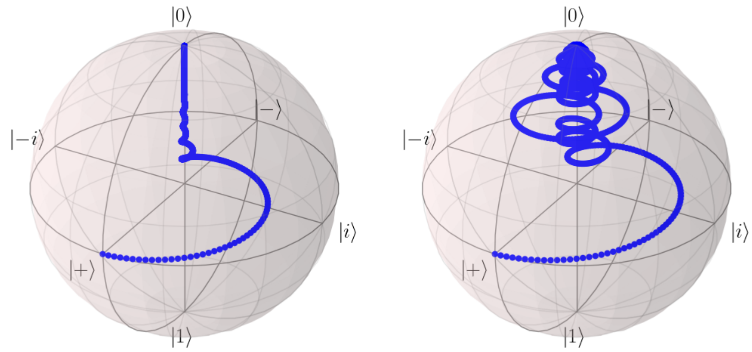

FIG. 7. From left to right: Qubit Evolution due to LME, Qubit Evolution due to RME

[2] J. Preskill, Quantum computing in the nisq era and beyond, Quantum **2**, 79 (2018).

[3] P. Bertet, J. Gambetta, D. Schuster, J. Majer, M. Devoret, S. Girvin, and R. Schoelkopf, Trimon: A qubit system designed for studying quantum information, Physical Review B **72**, 054503 (2005).

[4] E. Paladino, Y. Galperin, G. Falci, and B. Altshuler, Decoherence in solid-state qubits, Reviews of Modern Physics **86**, 361 (2014).

[5] J. Koch, T. M. Yu, J. Gambetta, A. Houck, D. Schuster, J. Majer, A. Blais, M. Devoret, S. Girvin, and R. Schoelkopf, Charge-insensitive qubit design derived from the cooper pair box, Physical Review A **76**, 042319 (2007).

[6] H.-P. Breuer and F. Petruccione, *The Theory of Open Quantum Systems* (Oxford University Press, 2002).

[7] Y.-P. Liu, Y. Chen, H.-X. Zhang, H.-O. Li, G.-Q. Chen, and G.-C. Guo, Charge noise induced decoherence in a fluxonium-trimon hybrid qubit, Journal of Applied Physics **128**, 214503 (2020).

[8] H.-P. Breuer and F. Petruccione, An open systems approach to quantum optics, Lectures in Theoretical Physics **1** (1999).

[9] T. Roy, Multimode superconducting circuits as building blocks for a programmable quantum processor (2018).

[10] Y. Chen, Y.-P. Liu, H.-X. Zhang, H.-O. Li, G.-Q. Chen, and G.-C. Guo, Trimon-type superconducting circuit architecture for scalable quantum computing, npj Quantum Information **7**, 1 (2021).

[11] D. A. Lidar, Lecture notes on the theory of open quantum systems (2020), arXiv:1902.00967 [quant-ph].

[12] J. Gambetta, A. Blais, M. Boissonneault, A. MacDonald, S. Ashhab, and S. Girvin, Qubit-oscillator systems, Physical Review A **77**, 012112 (2008).

[13] F. Yan, S. Gustavsson, A. Kamal, J. Birenbaum, A. P. Sears, A. Sirois, S. Weber, K. Osborn, J. Gambetta, and W. Oliver, Fluxonium qubit under the influence of realistic charge noise, Physical Review B **93**, 184506 (2016).

[14] H.-P. Breuer and F. Petruccione, The theory of open quantum systems, (2002).

[15] V. May and O. Kühn, Theoretical treatment of the dynamics of excitation energy transfer, Chimia **26**, 385 (1972).

[16] N. Lambert, T. Raheja, S. Cross, P. Menczel, S. Ahmed, A. Pitchford, D. Burgarth, and F. Nori, QuTiP-BoFiN: A bosonic and fermionic numerical hierarchical-equations-of-motion library with applications in light-harvesting, quantum control, and single-molecule electronics, Physical Review Research **5**, 10.1103/physrevresearch.5.013181 (2023).

[17] J. R. Johansson, P. D. Nation, and F. Nori, Qutip 2: A python framework for the dynamics of open quantum systems, Computer Physics Communications **184**, 1234 (2013).

[18] A. Ishizaki and Y. Tanimura, Quantum dynamics of system strongly coupled to low-temperature colored noise bath: Reduced hierarchy equation approach, The Journal of chemical physics **123**, 234505 (2005).

[19] X. Wang, A. Tokmakoff, and M. Fayer, Non-markovian evolution of the density operator in the presence of strong laser fields, The Journal of chemical physics **111**, 8906 (1999).

[20] T. Matsubara, A new approach to quantum-statistical mechanics, Progress of Theoretical Physics **14**, 473 (1955).

[21] E. P. Rosenthal, Approaches to modeling and simulation of superconducting circuits, arXiv preprint arXiv:1802.06944 (2018).

[22] A. J. Leggett, S. Chakravarty, A. Dorsey, M. P. Fisher, A. Garg, and W. Zwerger, Dynamics of the dissipative two-state system, Reviews of Modern Physics **59**, 1 (1987).

[23] C. W. Gardiner and P. Zoller, Quantum noise, Springer Series in Synergetics **56** (2004).

[24] H.-P. Breuer and F. Petruccione, On the time-convolutionless projection operator technique, Annalen der Physik **9**, 517 (2000).

[25] G. Lindblad, On the generators of quantum dynamical semigroups, Communications in Mathematical Physics **48**, 119 (1976).

[26] H. Chen and D. A. Lidar, Hamiltonian open quantum system toolkit, Communications Physics **5**, 1 (2022).